Article

Not peer-reviewed version

Late Bone Marrow Mononuclear Cell Transplantation in Rats with Sciatic Nerve Crush. Analysis of a Potential Therapeutic Time Window.

Vanina Usach , Mailin Casadei , Gonzalo Piñero , Marianela Vence , Paula Soto , Alicia Cueto , Pablo Brumovsky , Clara Patricia Setton-Avruj *

Posted Date: 7 May 2024

doi: 10.20944/preprints202405.0352.v1

Keywords: Bone marrow mononuclear cells; sciatic nerve crush; transplantation; neuropathic pain; regeneration

Article

Late Bone Marrow Mononuclear Cell Transplantation in Rats with Sciatic Nerve Crush. Analysis of a Potential Therapeutic Time Window

Vanina Usach [1,2], Mailin Casadei [3], Gonzalo Piñero [1,2], Marianela Vence [2], Paula Soto [1,2], Alicia Cueto [4], Pablo Brumovsky [3] and C. Patricia Setton-Avruj [1,2,*]

[1] Universidad de Buenos Aires. Facultad de Farmacia y Bioquímica. Departamento de Química Biológica. Cátedra de Química Biológica Patológica. Ciudad Autónoma de Buenos Aires, Argentina.; vaninausach@gmail.com, gonzalopiniero@gmail.com, paula.asoto02@gmail.com

[2] Universidad de Buenos Aires-CONICET. Instituto de Química y Fisicoquímica Biológicas (IQUIFIB). Ciudad Autónoma de Buenos Aires, Argentina; vencemarianela@yahoo.com.ar

[3] Instituto de Investigaciones en Medicina Traslacional (IIMT) – CONICET – Universidad Austral; maicasedei@hotmail.com, pbrumovs@austral.edu.ar

[4] Servicio de Neurología, Hospital Español de Buenos Aires, Buenos Aires, Argentina; alicueto@gmail.com

* Correspondence: setton@qb.ffyb.uba.ar; Tel.: (+54 11) 4964 8287

Abstract: After peripheral nerve injury, axon and myelin regeneration are key events for optimal clinical improvements. We have previously shown that early bone marrow mononuclear cell (BMMC) transplantation exerts beneficial effects on myelin regeneration. In the present study we analyze whether there is a temporal window in which BMMC migrate more efficiently to damaged nerves while still retaining their positive effects. Adult Wistar rats of both sexes, with sciatic nerve crush were systemically transplanted with BMMC at different days post injury. Vehicle-treated, naïve, and sham rats were also included. Morphological, functional, and behavioral analyses were performed in nerves from each experimental group at different survival times. BMMC transplantation between 0 and 7 days after injury resulted in the largest number of nested cells within the injured sciatic nerve, which supports the therapeutic value of BMMC administration within the first week after injury. Most importantly, later BMMC administration 7 days after sciatic nerve crush was associated with neuropathic pain reversion, improved morphological appearance of the damaged nerves, and a tendency toward faster recovery in the sciatic functional index and electrophysiological parameters. Our results thus support the notion that even delayed BMMC treatment may represent a promising therapeutic strategy for peripheral nerve injuries.

Keywords: Bone marrow mononuclear cells; sciatic nerve crush; transplantation; neuropathic pain; regeneration

1. Introduction

Peripheral nerve injury is typically associated with Wallerian degeneration both at and distal from the site of injury[1]. Various types of infiltrating immune cells participate in debris removal[2,3] and clearance of partially damaged axons[4], causing variable alterations in limb sensitivity, functional loss, and neuropathic pain[5,6].Because axonal regeneration and remyelination are key events for optimal clinical improvement, finding relevant therapeutic strategies is of great importance.

Stem cell therapy has emerged as a promising approach in the field of regenerative medicine[7,8]. Particularly, bone marrow mononuclear cells (BMMC) have appeared as a suitable option because of their convenient isolation protocol, high yield and survival rate after transplantation, and low immunogenicity[9]. Their therapeutic potential has been addressed in several animal models of injuries[10–16]. BMMC are capable of stimulating neovascularization[17] or re-epithelialization and wound healing[18]; and their therapeutic value has been further studied in several recent clinical trails[19–26]. We have previously shown in rat models of irreversible[27] and

 doi:10.20944/preprints202405.0352.v1

reversible Wallerian degeneration[8,28] that BMMC migrate almost exclusively to the injured site. Interestingly, the administration of BMMC immediately after sciatic nerve crush promotes considerable regeneration in nerve and myelin, partial recovery of electrophysiological properties, and the complete prevention of associated neuropathic pain[8].

However, the question remains whether there is an optimal temporal window for BMMC administration after injury. In animal models of myocardial infarction, it has been shown that the most beneficial results are obtained when transplantation occurs during the acute phase[11,29]. Studies in humans also point at a temporal window when BMMC transplant is most effective, as early interventions in patients suffering traumatic paraplegia resulted in better clinical outcomes[25]. Of note, a time window of therapeutic opportunity for the use of BMMC in animals undergoing peripheral nerve injury has not been established yet.

Here, we aimed at determining the temporal window in which transplanted BMMC migrate most efficiently in a model of sciatic nerve crush, and whether this administration results in similar behavioral, morphological, and physiological improvements as those previously observed[8]. The results obtained in the present manuscript support the notion that even delayed BMMC treatment may represent a promising therapeutic strategy for peripheral nerve injuries.

2. Results

2.1. Kinetics of BMMC Migration

We observed the largest number of nested ^{EGFP}BMMC in the distal area of the ipsilateral (IL) nerve in rats transplanted between 0-7 dpi, with significant differences from naïve rats but not between early and late transplant (Figure 1a and 1b). Transplant 14 dpi and onward showed a marked decrease in the number of recruited cells, which resulted in no significant differences from naïve rats (Figure 1a). Virtually no ^{EGFP}BMMC were detected in naïve, contralateral (CL) nerves or the proximal stump of IL nerves (Figure 1a and 2b).

Considering the results obtained, we chose 7 dpi transplant to address the effects of late BMMC administration on the function and morphology of injured nerves.

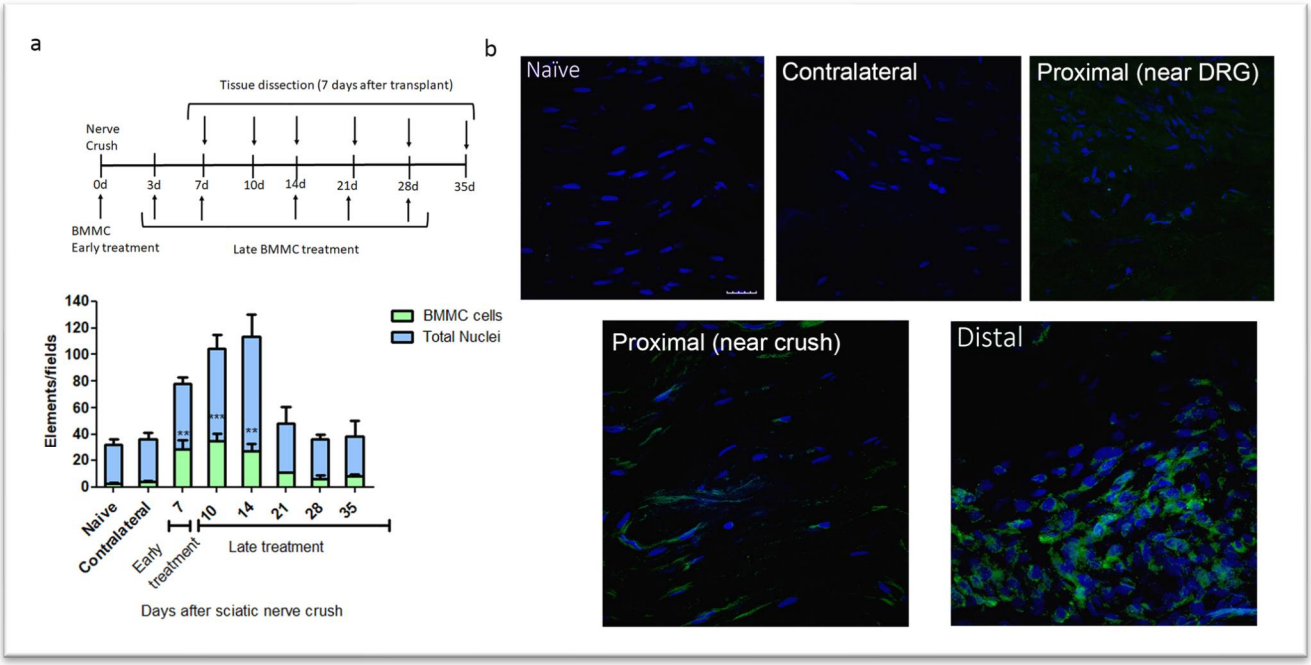

Figure 1. Kinetics of BMMC migration (n=5, 60X, scale bar: 10 μm). a: Experimental design indicating ^{EGFP}BMMC transplant and tissue collection times. For all time-points, animals were sacrificed 7 days post-transplant: Bar graph showing total nuclei (blue) and ^{EGFP}BMMC (green) per field in naïve and distal areas of IL nerves at different days post injury. Values are expressed as mean ± SD. Statistical analysis performed through one way-ANOVA followed by Dunnett's post-hoc test. *p<0.05, ***p<0.001 (^{EGFP}BMMC on different days post injury vs. naïve). **b:** Representative confocal microscopy images of a naïve, contralateral, proximal near DRG, proximal near crush and distal area

 doi:10.20944/preprints202405.0352.v1

of an ipsilateral nerve 14 days post injury showing DAPI-positive nuclei (blue) and transplanted ^{EGFP}BMMC (green).

2.2. Effects of late BMMC Transplant on Mechanical and Cold Allodynia

All injured rats exhibited a progressive decrease in IL mechanical withdrawal thresholds and an increase in cold withdrawal frequency and score during the first 7 dpi (Figure 2). Vehicle-treated animals maintained IL mechanical allodynia until 21dpi, followed by a slow recovery that was only complete 35dpi. In contrast, late BMMC-treated rats showed a progressive increase in IL mechanical withdrawal threshold starting 8 dpi and considerable improvement during the first week after transplant, reaching basal withdrawal levels 21 dpi and onward (Figure 2a).

Analysis of cold allodynia showed that vehicle-treated rats maintained significant increases in IL cold withdrawal frequency (Figure 2b top panel) and score (Figure 2b bottom panel), both returning to basal levels 35dpi. At variance, late BMMC transplant resulted in a sharp reduction in IL cold allodynia over the first week after transplant, with animals exhibiting basal cold withdrawal frequency (Figure 2b top panel) and score (Figure 2b bottom panel) as soon as 21 dpi.

Neither vehicle-treated nor late BMMC-treated rats exhibited noticeable changes in CL mechanical withdrawal threshold or cold withdrawal frequency and score throughout the study (Figure 2).

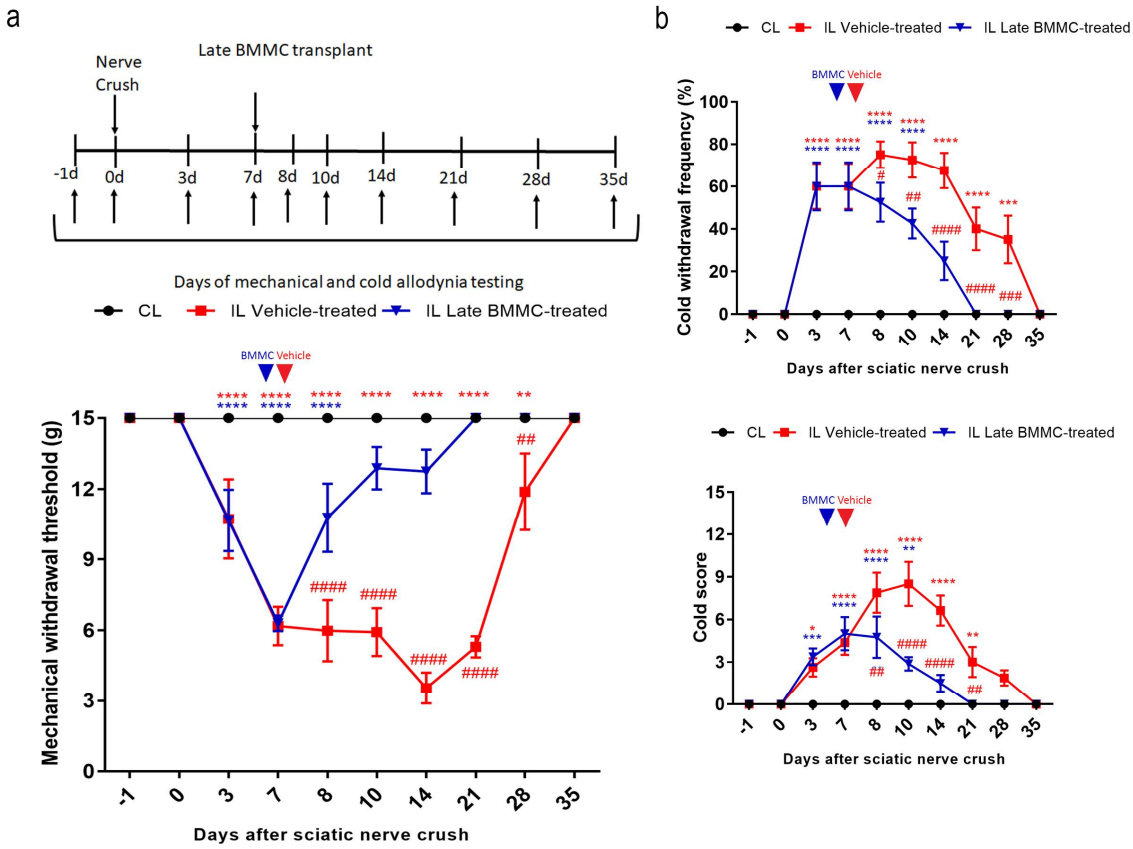

Figure 2. Effects of late BMMC transplant on mechanical and cold allodynia (n=8). a: Experimental design showing sciatic nerve crush, transplant and pain-like behavioral test times. Mechanical withdrawal threshold calculated as 50% g threshold = (10 Xf+kd)/10000, where Xf = value (in log units) of the final von Frey hair used; k = tabular value for the pattern of positive/negative responses; and d = mean difference (in log units) between stimuli. **b:** Cold withdrawal frequency calculated as (N° of trials accompanied by brisk foot withdrawal) x 100 / (N° of total trials); cold withdrawal score: 0 = no response, 1 = quick withdrawal, flick or stamp of the paw; 2 = prolonged withdrawal or repeated flicking (≥2) of the paw; 3 = repeated flicking of the paw with licking directed at the ventral side of the paw. Results corresponds to contralateral (CL, black circle) pools data from vehicle-treated and

 doi:10.20944/preprints202405.0352.v1

late BMMC-treated rats and ipsilateral (IL) hind paws of vehicle-treated (red square) and late BMMC-treated rats (blue triangles). Values are expressed as mean ± SD. Blue arrows indicate the time-point of vehicle or BMMC administration. Statistical analysis performed through two-way ANOVA followed by Bonferroni post-hoc test. p<0.0001 among groups in B and C; ## p<0,001, ### p<0,001, #### p<0,0001 (IL vehicle-treated vs. IL late BMMC-treated); red * p<0,05, ** p<0,001, *** p<0,001, **** p<0,0001 (IL vehicle-treated vs. CL); blue ** p<0,001, *** p<0,001, **** p<0,0001 (IL late BMMC-treated vs. CL). .

2.3. Effects of Late BMMC Treatment on SFI, Distal Latency and CMAP

Both experimental groups exhibited similarly altered footprints at 7 and 14 dpi; none of the toes were evident (Figure 3a right top panel), and a significant reduction was observed in SFI and footprint area (Figure 3a bottom panel). At 21 dpi, vehicle-treated rats showed undifferentiated 2nd-4th toe prints and a significant decrease in SFI compared to naïve and BMMC-treated rats (Figure 3a) and in footprint area compared to naïve rats (Figure 3a bottom panel). At 28 dpi, all toes showed a separate print and the SFI was not significantly different from naïve rats (Figure 3a bottom panel); however, the hind paw area was smaller than that observed in naïve animals. In contrast, a clear print was observed for all toes in BMMC-treated rats starting 21 dpi (Figure 3a right top panel), and the SFI and hind paw area (Figure 3a bottom panel) exhibited values similar to naïve rats.

Distal latency showed a significant increase in both experimental groups from 7 dpi and up to 28 dpi, with no statistically significant differences between them (Figure 3b). However, a tendency toward a faster but not significant recovery was noticed in late BMMC-transplanted rats35 dpi.

Analysis of CMAP amplitude in vehicle-treated rats showed a reduction in amplitude values from 7 to 21 dpi, followed by a partial recovery 28 dpi and full recovery with basal values 35 dpi (Figure 3b). BMMC-treated rats exhibited a similar CMAP amplitude change as compared to vehicle-treated rats, although a significant increase was only detected as from 21 dpi (Figure 3b).

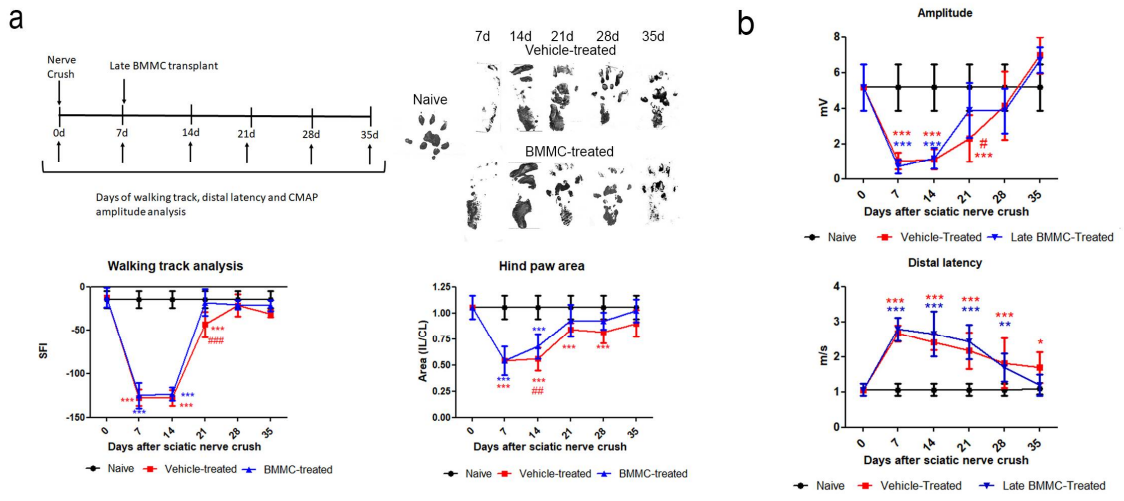

Figure 3. Effects of late BMMC transplant on SFI, distal latency and CMAP (n=6). a: Experimental design showing sciatic nerve crush, transplant, and test times. Representative ipsilateral hind paw; sciatic functional index analysis (SFI) and ipsilateral/contralateral (IL/CL) hind paw area of naïve, vehicle- and BMMC-treated rats. **b:** CMAP amplitude and distal latency of naïve, vehicle-and BMMC-treated rats. Values are expressed as mean ± SD. Statistical analysis performed through two-way ANOVA followed by Bonferroni's post-hoc test. *p<0,05; ***p<0,001 (vehicle-treated or BMMC-treated vs. naïve); #p<0,05; ##p<0,01; ###p<0,001 (vehicle-treated vs. BMMC-treated). .

2.4. Effects of Late BMMC Transplant on Axon Number and Remyelination State

The analysis of semi-thin sections of sciatic nerves from naïve animals showed healthy axons, most of them of large caliber (Figure 4a.1 arrows). Conversely, analysis at 7 dpi revealed axon and myelin debris characteristic of Wallerian degeneration (Figure 4a.2 asterisk). As survival time proceeded, vehicle-treated animals 14 dpi exhibited axon and myelin debris (Figure 4b, asterisk) and

 doi:10.20944/preprints202405.0352.v1

newly synthesized axons of small caliber (Figure 4b, arrowhead). Studies at 21 dpi showed no myelin or axon debris but small newly formed axons (Figure 4c). Finally, most axons resembled those of naïve rats at 28 dpi, although with fewer myelin layers (Figure 4d, arrow). In contrast, the BMMC-treated group barely showed myelin or axon debris 14 dpi (Figure 4f, asterisk) but revealed a large number of newly synthesized axons of small caliber (Figure 4f, arrowhead). Beginning at 21 dpi, axon caliber increased and reached a naïve-like phenotype (Figure 4g and h, arrows).

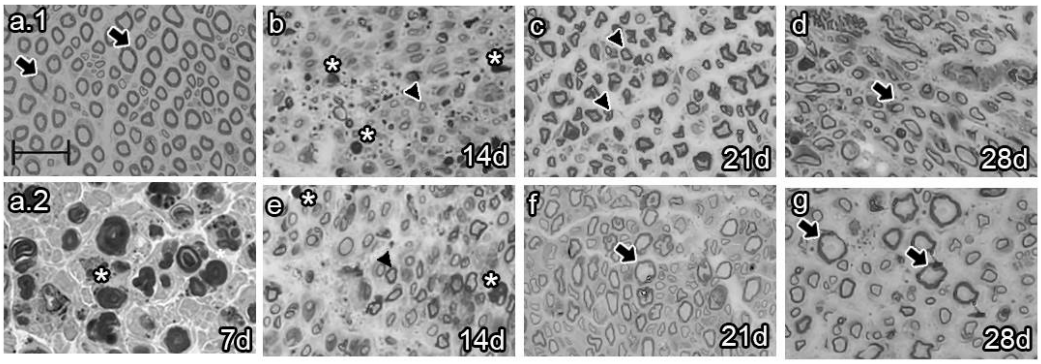

Figure 4. Semi-thin section analysis of late BMMC transplant (n=3, 40X, scale bar 20 μm). Analysis of naïve (a.1), vehicle-treated (a.2-D) and BMMC-treated rats (e-g) at different survival times. Arrows indicate healthy axons, asterisks indicate myelin and axon debris, arrowheads indicate newly formed axons.

Ultrastructural analyses of sciatic nerves (Figure 5) showed mostly myelinated axons of large caliber in naïve animals (Fig, 5a.1, arrows). Seven and 14 dpi, vehicle-treated animals only showed degenerating axons and myelin debris (Figure 5a.2 and b, hashtag and asterisk, respectively). Myelin and axon debris disappeared at 21 dpi, and newly formed myelinated axons were observed of large caliber and unusual shape (Figure 5c). As spontaneous regeneration proceeded, axons of large caliber with a thin myelin layer and naïve-like shape were observed at 28 dpi (Figure 5d, arrow). In turn, the BMMC-treated group showed some myelinated axons of large caliber wrapped by a thin myelin layer at 14 dpi (Figure 5f, arrow heads). Axons became more myelinated at 21 dpi and acquired a normal myelin sheath and shape at 28 dpi (Figure 5g and h, arrows).

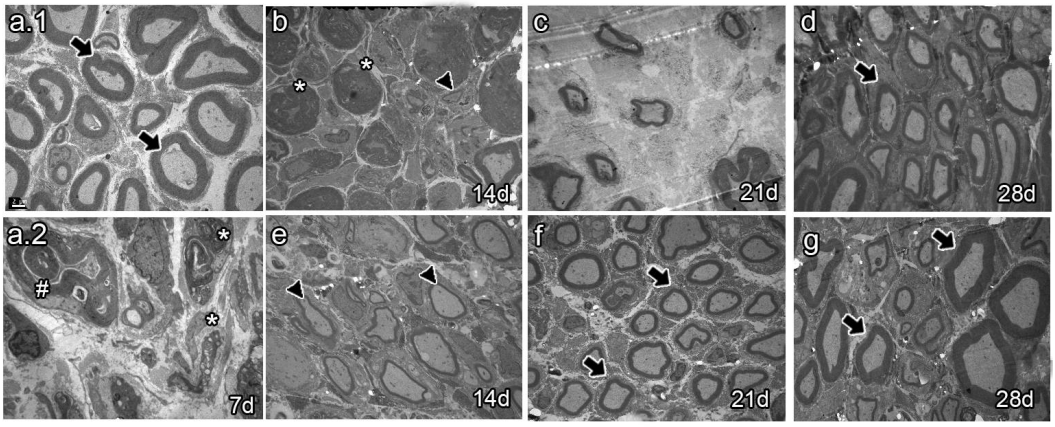

Figure 5. Ultrastructure analysis of late BMMC transplant (n=3, 3000X, scale bar 2 μm). Analysis of naïve (a.1), vehicle-treated (a.2-d) and BMMC-treated rats (e-g) at different survival times. Asterisks indicate myelin debris; hashtags indicate newly formed axons.

As regards axon quantification, results in figure 6 show a sharp decrease in the total number of axons as from 7 dpi in the vehicle-treated group (15,32 ± 6.4 %) and a return to normal values 28 dpi (102 ± 14.8 %). In the BMMC-treated group, the total number of axons began to increase as from 7dpi –the day of BMMC transplant– and reached values non-significantly different from naïve nerves at 21 dpi (86 ± 3.46 %).

 doi:10.20944/preprints202405.0352.v1

Digging deeper into axon number and remyelination, we found a sharp decrease in the number of large-caliber myelinated axons 7dpi in the vehicle-treated group (16.6 ± 10.5 %) and a return to normal values 28 dpi (95 ± 5%). In contrast, the BMMC-treated group evidenced a marked recovery in the number of large-caliber myelinated axons as from 14 dpi (74.66 ± 3.28 %), with values non-significantly different from naïve nerves. Small-caliber axons increased in number in the vehicle-treated group at 7 dpi (100 %) and gradually decreased until normal values at 28 dpi (5 ± 5 %). In contrast, the BMMC-treated group revealed a sharp decrease in the number of small-caliber axons as from 14 dpi (25.33 ± 3.28 %), once again with values non-significantly different from naïve nerves.

Regarding the g-ratio (Figure 6b), an increase was observed in vehicle-treated animals 7dpi as compared to naïve animals (0.75 ±0.08). The g-ratio remained high up to 28 dpi in the vehicle-treated group but recovered normal values as from 21 dpi in the BMMC-treated group (0.60±0.1). The number of myelin layers per 100 nm decreased at 7dpi in vehicle-treated rats (8.69 ± 0.58) and remained significantly different from naïve nerves until 28 dpi (9.98 ± 0.78); in the BMMC-treated group, no significant differences were observed from naïve nerves as from 14 dpi (9.76 ± 0.52). Finally, the intraperiod line revealed significant differences only at 14 and 21 dpi (10.19 ± 1.4 and 9.73 ± 1.4) in sciatic nerves from animals in the vehicle-treated group.

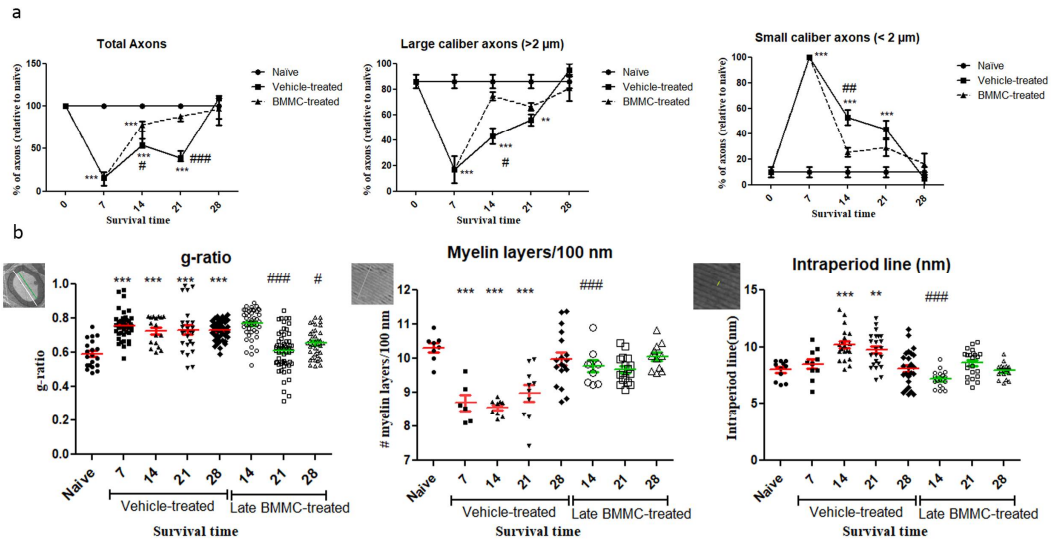

Figure 6. Ultrastructure quantification (n=3): a: Quantification of total axons/30 µm², percentage of large- and small-caliber axons in vehicle-treated and late BMMC-treated rats at different dpi. Values are expressed as the mean ± SD. Statistical analysis performed through two-way ANOVA followed by Bonferroni's post-hoc test. * p<0.05; **p<0,01; ***p<0,001 (vehicle-treated or BMMC-treated vs. naïve rats); # p<0,05; ##p<0.01; ### p<0.001 (vehicle-treated vs. BMMC-treated rats). **b**: Quantification of g-ratio, myelin layers/100 nm and intraperiod line length in vehicle-treated and late BMMC-treated rats at different dpi. Schematic images showing how each parameter in panel B was measured: for g-ratio, the green line represents axon diameter; the white line represents axon plus myelin diameter; for myelin layers, the line represents 100 nm and for intraperiod lines the line indicates it. Values are expressed as the mean ± SD. Statistical analysis performed through one-way ANOVA followed by Bonferroni's post-hoc test. *p<0.05; **p<0,01; ***p<0,001 (vehicle-treated or BMMC-treated vs. naïve rats), # p<0,05; ##p<0.01; ### p<0.001 (vehicle-treated vs. BMMC-treated rats).

2.5. Effects of Late BMMC Transplant on MBP and βIII-Tubulin Protein Levels and Distribution

Blotting analysis revealed a clear decrease in MBP levels in the distal stump of vehicle-treated rats (Figure 7a); with considerably low protein levels at 28 dpi (Figure 7b). Of note, a much smaller decrease was observed in late BMMC-treated rats (Figure 7a, b). In fact, significant differences were observed between experimental groups at all time-points evaluated (Figure 7b). βIII-tubulin levels also showed a decrease 14 and 21 dpi in vehicle-treated rats, followed by a substantial recovery 28 dpi (Figure 7a, b). In contrast, late BMMC transplant partially prevented the decrease in βIII-tubulin levels, only rendering slight statistically significant differences 14 and 21 dpi (Figure 7b).

 doi:10.20944/preprints202405.0352.v1

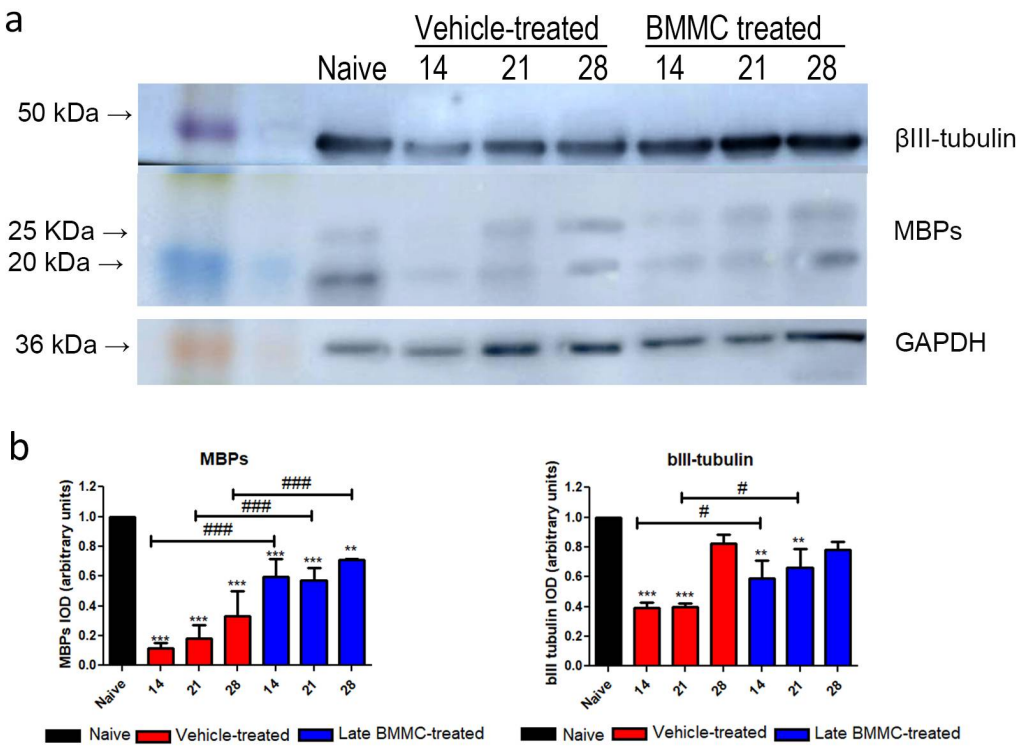

Figure 7. Immunoblot effects of late BMMC transplant on MBP and βIII-tubulin protein levels and distribution (n=3). a: Representative western blot image of a naïve nerve, and the distal area of ipsilateral nerves of vehicle- and BMMC-treated rats for βIII-tubulin (~50kDa) and MBP (~ 21 and 18.5 kDa). Rainbow molecular weight marker is shown on the left. **b:** Quantification of MBP and βIII-tubulin integrated optical density (IOD) normalized to GAPDH (~36kDa) levels and expressed relative to naïve nerves (AU, arbitrary units). In all cases, values are shown as mean ± SD. Statistical analysis performed through two-way ANOVA followed by Bonferroni's post-hoc test. **p<0,01; ***p<0,001 (vehicle-treated or BMMC-treated vs. naïve rats); # p<0,05 ### p<0,001 (vehicle-treated vs. BMMC-treated rats).

Immunohistochemical analysis confirmed the immunoblotting results. Thus, while MBP-like immunoreactivity (LI) in naïve nerves always produced a continuous and homogenous signal with an organized number of nuclei, sciatic nerve crush resulted in clear signs of demyelination, with a profound decrease in MBP-LI and the appearance of MBP clusters 7 and 14 dpi (Figure 8 asterisks), and also a significant increase in total nuclei, which became disorganized. BMMC treatment at both time points improved MBP-LI signal and reduced the number of clusters as compared to the vehicle-treated group; however, these effects were sharper in early BMMC-treated rats. Moreover, late BMMC-treated rats showed signs of improvement in MBP-LI as early as 14 dpi with the presence of MBP clusters accompanied with neosynthesized fibers (Figure 8 hashtag), and onward accompanied with reduction in number of total nuclei and recover of their organization (Figure 8 and 10a). The effect of late BMMC treatment on the demyelination process was confirmed through p75NTR-LI, a marker of repairing Büngner SC (data not shown).

 doi:10.20944/preprints202405.0352.v1

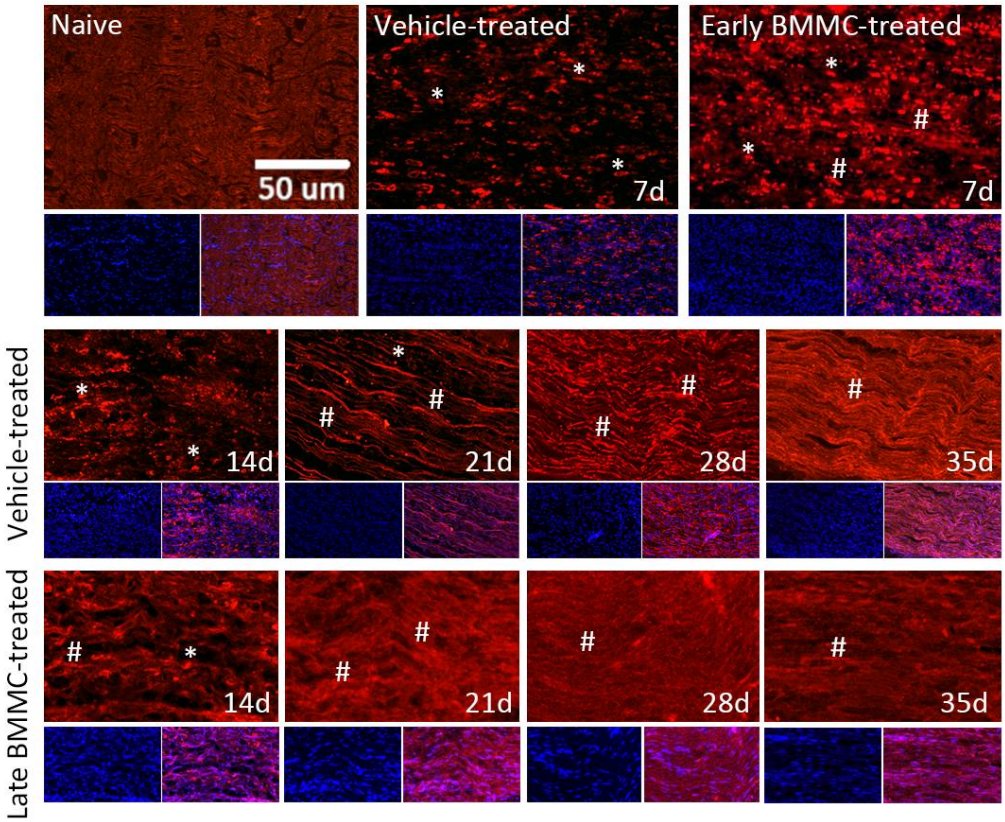

Figure 8. Immunohistochemical effects of late BMMC transplant on MBP-like immunoreactivity (n=5, 20X, scale bar 50 μm). Longitudinal sections from naïve nerves and the distal area (3-6 mm after crush) of vehicle- and early BMMC-treated animals analyzed 7 dpi. Middle and bottom panels show results obtained in the distal stump of vehicle- and late BMMC-treated rats evaluated at different dpi. In blue, DAPI immunostaining for nuclei and in red MBP immunostaining. Asterisks indicate MBP clusters and hashtags indicate newly synthetized myelin.

Finally, immunohistochemical analysis of axonal marker βIII-tubulin (Figure 9 and 10b) revealed that, compared to the homogenous signal observed in naïve rats, vehicle-treated rats exhibited a considerable decrease in βIII-tubulin-LI up to 14dpi, as well as the appearance of βIII-tubulin clusters (Figure 9 asterisks). In contrast, late BMMC-treated rats exhibited a noticeably smaller drop in βIII-tubulin-LI and cluster formation, with signs of significant improvement as from 14 dpi (Figure 9 hashtags). The quantity and organization of total nuclei had the same pattern as the one described in figure 8.

Preprints.org (www.preprints.org) | NOT PEER-REVIEWED | Posted: 7 May 2024 doi:10.20944/preprints202405.0352.v1

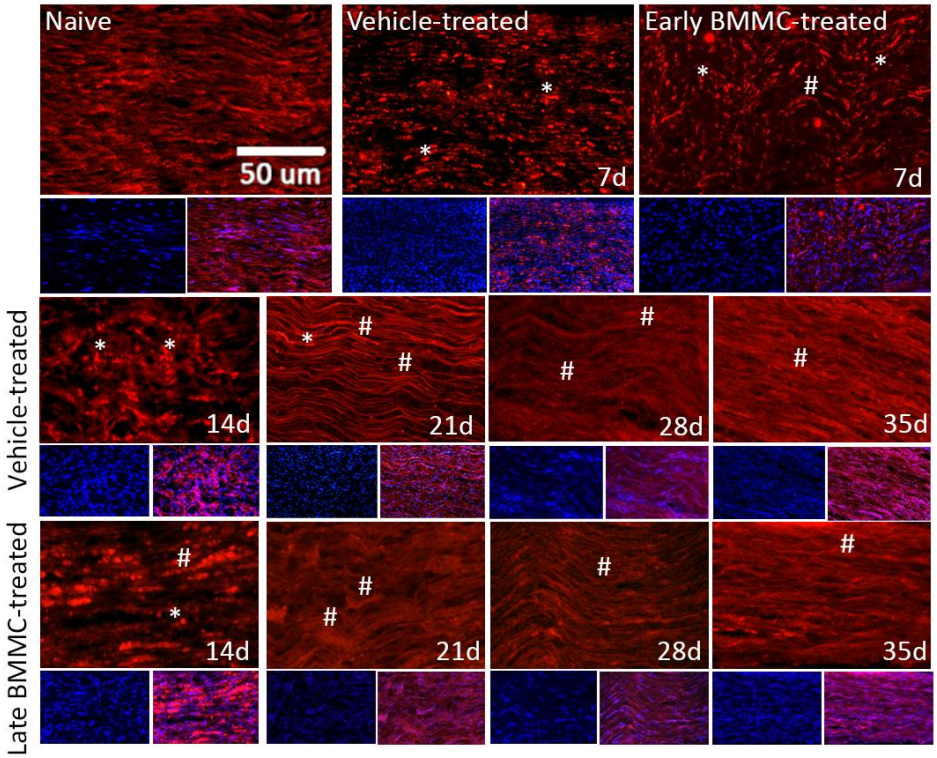

Figure 9. Immunohistochemical effects of late BMMC transplant on βIII-tubulin-like immunoreactivity (n=5, 20X, scale bar 50 µm). Longitudinal sections from naïve nerves and the distal area (3-6 mm after crush) of vehicle- and early BMMC-treated animals analyzed 7 dpi. Sections from the distal area of ipsilateral nerves of vehicle- and late BMMC-treated rats analyzed at different dpi. In blue, DAPI immunostaining for nuclei and in red βIII-tubulin immunostaining. Asterisks indicate βIII-tubulin clusters and hashtags indicate newly synthetized myelin.

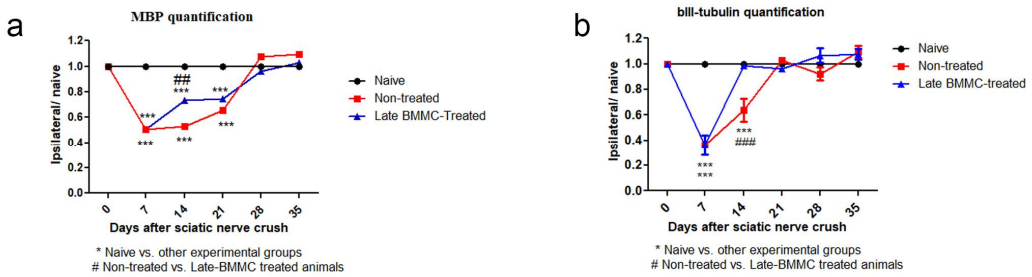

Figure 10. IOD quantification of MBP (a) and βIII-tubulin (b) (n=5). IOD quantification shown as the mean ± SEM relative to naïve nerves. Statistical analysis performed through two-way ANOVA followed by Bonferroni's post-hoc test. * p<0.05; **p<0,01; ***p<0,001 (naive vs. other experimental groups); # p<0,05; ##p<0.01; ### p<0.001 (vehicle-treated vs. late BMMC-treated animals). Significance was set at p<0.05.

3. Discussion

The present study supports the therapeutic value of systemic BMMC transplantation at a time when peripheral neuropathy is already installed. Transplant within the first 7 dpi in rats resulted in the most efficient cell recruitment, while later injections showed considerable reductions in BMMC infiltration. These observations are in line with the peak in total nuclei, indicating high Schwann cell (SC) proliferation and a rise in infiltrating inflammatory cells, both hallmarks of the Wallerian degeneration process[30–32]. BMMC administration 7 dpi efficiently reduced mechanical and cold allodynia and induced a faster recovery in the total number of axons, their myelination state, and the

 doi:10.20944/preprints202405.0352.v1

levels and organization of MBP and βIII-tubulin. A tendency toward accelerated functional recovery was also observed as from 14 dpi in terms of CMAP amplitude and SFI.

Analyses establishing the temporal window with the highest therapeutic impact of BMMC transplantation after injury remain scarce. Several authors have demonstrated beneficial effects in intravenous BMMC transplant models with transplant occurring between 1h and 7dpi[33–35]; however, no beneficial effects were obtained when transplant occurred 14 or 30 dpi[35]. Although fast therapeutic actions are key in inducing recovery, safe and beneficial effects have also been shown in dogs with chronic spinal cord injury[36,37] and rats with chronic stress[38]and depression[39].

Upon injury, SC actively proliferate, acquire a repair phenotype[40,41]and secrete trophic factors and cytokines that promote neuronal survival and leukocyte influx[31]. This microenvironment facilitates the signaling, migration and nesting of a variety of immune cells[42–44], and the activation of resident mesenchymal precursors[45] or dedifferentiated SC with a mesenchymal cell-like phenotype[46]. This pro-regenerative, inflammatory microenvironment present in the sub-acute phase is essential to the recruitment of endogenous immune cells[47] and transplanted BMMC[48,49]. No significant migration was observed in the spontaneous regeneration phase, which suggests a much lesser chemoattractant environment as pro-inflammatory signals decrease.

Worth mentioning, late BMMC transplant was highly efficient in reducing and even eliminating pain-like behavior in injured rats. This finding agrees with previously published studies demonstrating that unilateral injection of BMMC into several muscles in rats with diabetic neuropathy ameliorates mechanical and cold hyperalgesia[50]and that early intravenous administration of BMMC completely prevents mechanical allodynia after sciatic nerve crush[8]. However, in mice with lumbar 5 spinal nerve injury, the intrathecal injection of BMMC 1 dpi resulted in a slight, although significant, increase in IL mechanical withdrawal threshold[51].

The mechanisms by which BMMC modulate neuropathic pain are yet to be determined. It has been proposed that their beneficial effects are associated with the variety of cells comprised in this population and their synergistic interactions[52,53]. The production of several cytokines[54]and the release of factors which can mediate potent antioxidant effects[55] have also been proposed as a potential mechanism of action. Interestingly, it has been determined that the upregulation of IL-6, IL-1β and TNF-α, among others[56,57], strongly influences neuropathic pain. It may be thus speculated that BMMC relieve neuropathic pain through an immunomodulatory action, previously described by our group, suppressing the expression of several pro-inflammatory cytokines and inducing anti-inflammatory cytokines and macrophage phenotype changes[51,58]. Taking in consideration our previous results about cytokine expression and other authors that demonstrated that some chemokines and neuroinflammation signaling are only upregulated in males in terms of neuropathic pain [59–61] , in the present manuscript male rats were only evaluated in terms of neuropathic pain. Also, female rats were excluded a estrous cycle introduces additional variability.

The SFI provides valuable information concerning the recovery of sensory-motor connections and cortical integration related to gait function after peripheral nerve injury[62].Previous reports established a clear correlation between the SFI, histomorphometric measurements and electrophysiological analysis[63,64]. However, our results do not actually support such a correlation, as also previously reported[65]. This discrepancy may be due to the severe nerve degeneration observed in the first 14 dpi and the difficulty in obtaining a reliable paw print[66]. Here, morphometric aspects showed an early response to treatment –evidenced by a recovery in axon number and myelin quantity and organization–, while improvements in functional properties were detected at later time-points. Worth highlighting, BMMC-treated rats exhibited SFI recovery 1 week earlier than vehicle-treated ones and a tendency toward accelerated recovery in CMAP amplitude, reflecting some correlation between histomorphometric and functional parameters.

Our results are also in line with clinical trials demonstrating the therapeutic value of BMMC. Patients with diabetic neuropathy have shown ameliorated pain and functional recovery in peripheral nerves, accompanied by increased nerve blood flow[50]. Chronic lymphedema patients revealed an improvement in limb circumference and walking abilities[25]. Also, children with cerebral palsy improved their gross motor function and spasticity 6 months after transplantation[67]. Finally, patients with spinal cord injury or chronic traumatic brain injury[49] receiving BMMC treatment exhibited significantly reduced functional deficits and became more independent in everyday tasks[48].

 doi:10.20944/preprints202405.0352.v1

4. Materials and Methods

4.1 Animals

All animals were treated humanely, and experimental procedures, including number of animals in each experiments, were performed following the guidelines of Comité de Bioética at Facultad de Farmacia y Bioquímica, Universidad de Buenos Aires (CICUAL 1488/19), the Institutional Animal Care and Use Committee (IACUC; 17-04) of the IIMT CONICET-Universidad Austral, and in accordance with the NIH Guide for the Care and Use of Laboratory Animals (NIH Publications 86-23), the Directive 2010/63/EU for animal experiments of the European Parliament and the Council of the European Union, taking in account the 3R principle (replace, reduce and refine). Adult wild type Wistar rats (^{WT}Wistar rats, 270-300 g) and transgenic background (enhanced green fluorescent protein-expressing ^{EGFP}Wistar rats, 300-350 g) of either sex were used except in behavioral studies where male ^{WT}Wistar rats were used. Animals were housed in a light- and temperature-controlled room with a 12-hour-light/dark cycle and access to food and water *ad libitum*. The transgenic strain was generously provided by Dr Mathieu (IQUIFIB-CONICET, Argentina) and Dr Pitossi (Fundación Instituto Leloir, Argentina).

4.2. Sciatic Nerve Crush

^{WT}Wistar rats were anesthetized intraperitoneally with ketamine (75 mg/kg) and xylazine (10 mg/kg), and their right sciatic nerve was exposed and crushed for 8s at mid-thigh level using jeweler's forceps[8,28].

4.3. BMMC Isolation and In Vivo Transplant

BMMC were isolated from femurs and tibias from ^{WT} or ^{EGFP}Wistar rats, as previously described[8,30]. Briefly, the bone marrow was extruded with DMEM+10% fetal calf serum (Cripion Biotecnologia Ltd., Buenos Aires, Argentina) and the aspirate was centrifuged through a Ficoll-Paque Plus (GE Healthcare#17-1440-02, Chicago, IL, USA) density gradient. The mononuclear cell fraction was used for further experiments[8,28,29].

Animals were transplanted at different days post injury (dpi; 0 [early treatment] or 3-28 days [late treatment]) with $1x10^7$ ^{EGFP}BMMC (for cell recruitment analysis) or ^{WT}BMMC (for effect analysis) through the lateral tail vein using a 21G needle[8,28]. Cell recruitment at the different survival times was analyzed using an Olympus FV1000 confocal microscope.

4.4. Experimental Groups

Animals were divided into vehicle- (DMEM) and BMMC-treated groups receiving treatment at different dpi and then sacrificed at different survival times (mentioned in each figure). Naïve and/or sham rats were also included. The number of animals used in each experiment is also indicated in each figure legend. All experimental procedures were done by researchers that were blind to experimental design in order to avoid bias.

4.5. Behavioral Testing

Animals were first acclimatized to the chambers or walking pathway in a quiet room during daytime before surgery and at different dpi, to evaluate the following tests:

4.6. Mechanical Allodynia

The mechanical withdrawal threshold was assessed using von Frey filaments of different bending forces (Stoelting Inc., Wood Dale, IL, USA). The center of the plantar surface of the IL and CL hind paws were mechanically stimulated, following the modified up-down method of Dixon[68], to establish the 50% withdrawal threshold. A paw withdrawal reflex obtained with 6.0 g force or less was considered an allodynic response.

4.7. Cold Allodynia

A drop of acetone was gently brought in contact with the plantar surface of both hind paws for5 times (once every 5 min) in each one[69]. For withdrawal frequency analysis, a positive response was scored as 1, and lack of withdrawal as 0. For cold sensitivity scoring, responses to acetone were

 doi:10.20944/preprints202405.0352.v1

graded using a previously described 4-point scale[70]. Cumulative scores were generated, with the minimum score being 0 and the maximum score being 15. Statistically significant increases in withdrawal frequency and cold sensitivity scoring in response to acetone were interpreted as cold allodynia.

4.8. Walking Track Analysis

Rats were placed in a walking pathway[71] and allowed to walk down the track after dipping their hind feet in non-toxic ink. At least 3 prints of each foot were obtained and used to calculate the sciatic functional index (SFI) and the area of the footprint (Figure 11a); a value of 0 indicates a completely healthy nerve, whereas a value of -100 indicates total impairment of sciatic function. The areas were outlined manually and calculated using ImageJ (Figure 11b), and the IL/CL ratio was then determined.

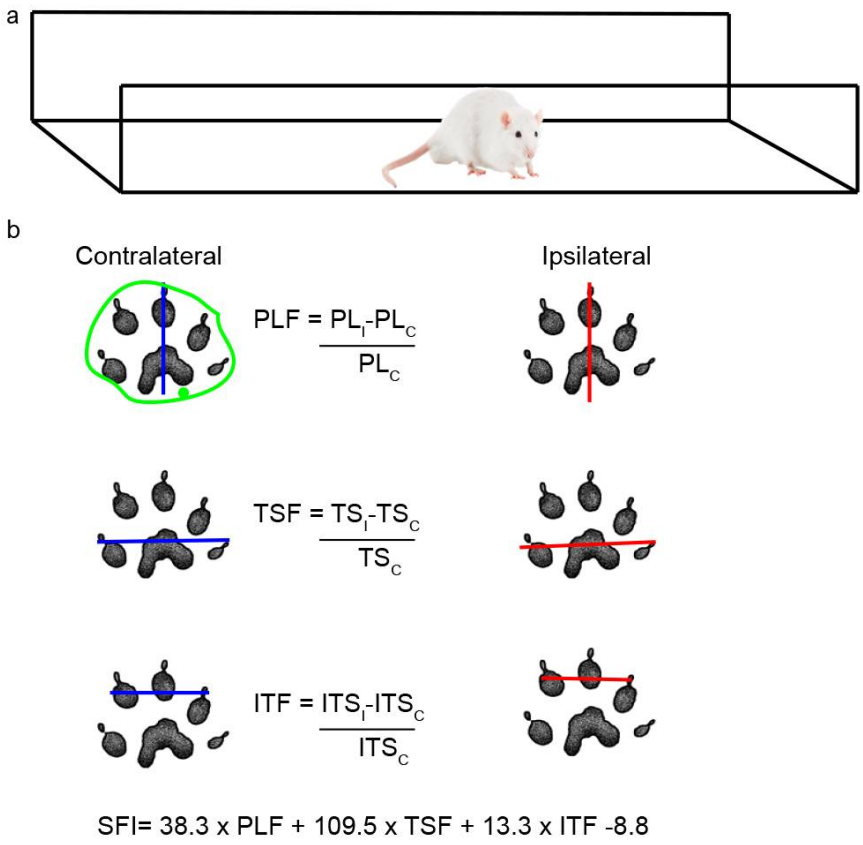

Figure 11. Scheme of walking track analysis. a: Acrylic walkway (120x15 cm, ending in a darkened cage) used for walking track analysis. **b:** In the footprint obtained, the length of the footprint from the third toe to the end of the foot (PL), the distance between the first and fifth toe (TS) and between the second and fourth toes (ITS) were measured in both the CL and IL sides. The green outline shows an example of how each area was determined.

4.9. Distal Latency and Compound Muscle Action Potential (CMAP) Recording

Both parameters were recorded in vehicle- and BMMC-treated rats at different dpi as previously described[8] using a portable electromyography instrument (Cadwell Wedge Sierra II, Cadwell Labs, Inc., Kennewick, WA, USA). Briefly, animals were anesthetized, and body temperature maintained at 37°C with a thermal blanket. Recording and ground electrodes were placed in the soleus muscle and the tail, respectively. The IL sciatic nerve was exposed, and the distal end electrically stimulated with 30 mA; a slight twitching of the limb was considered positive stimuli. The same procedure was carried out in naïve and CL nerves. The distal latency and the amplitude of the compound action potential (CMAP) were recorded.

 doi:10.20944/preprints202405.0352.v1

4.10. Electron and Optical Microscopy Analysis

Fourteen, 21 and 28 dpi, animals were anesthetized and perfused with 4% paraformaldehyde plus 2.5% glutaraldehyde in 0.1 M phosphate buffer, pH 7.4. The distal area of the ipsilateral nerve and a naïve sciatic nerve were dissected, and tissue was prepared as previously described[33]. Semi-thin tissue sections were mounted onto glass slides and dyed with 0.5% Toluidine blue in sodium carbonate 2.5% (w/v). Ultra-thin sections were collected on 300 mesh copper grids, dyed with 2% (w/v) aqueous uranyl, stained with Reynolds solution, and later analyzed in a Zeiss EM 109T electron microscope.

4.11. Western Blot Analysis

Naïve nerves and the distal stump (1.6 cm from the injured site) of IL nerves from vehicle- or BMMC-treated rats were dissected at different dpi and homogenized in TOTEX buffer containing protease inhibitor cocktail set III (Calbiochem- Milipore Sigma Chem Co. #535140, St Louis, MO, USA).

Proteins were quantified by means of Bradford's method[72], electrophoretically separated on 12.5% SDS-PAGE, and transferred onto polvinylidine fluoride membranes for immunoblotting. Membranes were incubated with primary antibodies (overnight, 4°C, Table 1a). After washing, membranes were incubated with horseradish peroxidase (HRP)-conjugated secondary antibodies (Table 1b) and developed using a chemiluminescent reagent (Biolumina, Kalium Technologies, Buenos Aires, Argentina) and the ImageQuant detector (LAS 500, GE Healthcare).

The relative intensity of myelin basic protein (MBP) and βIII-tubulin immunoreactive bands was analyzed using ImageJ software (National Institutes of Health, Bethesda, MD, USA) and normalized to GAPDH levels.

Table 1. A: Primary antibodies used for WB and IHC; **B:** Secondary antibodies used for WB and IHC.

Table 1 (a) Primary antibodies used for WB and IHC, (b) Secondary antibodies used for WB and IHC

Antigen	Cat #	Host	Clonality	Isotype (Clone)	Brand	Dilution	
						WB	IHC
Primaryantibodies							
MBP	800403	Mouse	Monoclonal	IgG_1 (SMI99)	Biolegend*	1:2500	1:1500
βIII-tubulin	802001	Rabbit	Polyclonal	Poly18020	Biolegend*	1:7500	1:2500
Loading control							
GAPDH	Ab-8245	Mouse	Monoclonal	IgG_1 (6C5)	Abcam**	1:5000	

Secondaryantibodies						
Reactivity	Cat #	Conjugate	Host	Brand	Dilution	
					WB	IHC
Mouse	115-035-146	HRP	Goat	Jackson ImmunoResearch***	1:10000	
Rabbit	111-035-003	HRP	Goat	Jackson ImmunoResearch***	1:8000	
Mouse	A11030	Alexa546	Goat	Thermofisher****		1:500
Rabbit	A21206	Alexa488	Donkey	Thermofisher****		1:500

* Biolegend, San Diego, CA, USA ** Abcam, Waltham, MA, USA; ***Jackson ImmunoResearch, West Grove, PA, USA ****Thermofisher, Carlsbad, CA, USA.

 doi:10.20944/preprints202405.0352.v1

4.12. Preparation of Tissue Sections and Immunohistochemistry

IL and CL nerves from injured rats at different dpi were prepared for immunohistochemistry, following previously described methods[8,28]. Slices were incubated with primary antibodies (overnight, 4°C, Table 1a) followed by incubation with secondary antibodies (Table 1b) plus DAPI (2 μg/ml, Sigma Chem Co). Tissues were mounted with Mowiol anti-fading solution for epifluorescence microscopy analysis using an Olympus BX100 epifluorescence microscope. Controls were done by incubating the samples without the primary antibody[73].[74].

4.13. Image Analysis

For migrating BMMC analysis, the number of recruited ^{EGFP}BMMC in the distal stump was evaluated 7 days post-transplant, comparing between early and late transplant at different dpi; naïve animals were used as control. In immunofluorescence studies, at least 5 animals per experimental group were analyzed. Ten images from each condition were processed from regions 1.2-1.5 cm before crush (proximal near dorsal root ganglia (DRG)), 3-6 mm before crush (proximal near crush) or 3-6 mm after crush (distal) in each IL nerve.

In semi-thin sections, the total number of axons per 100 μm^2 was calculated in 30 randomly selected fields. In ultra-thin sections, the total number of axons and those of small (< 2 μm diameter) and large (≥ 2 μm diameter) caliber per 30 μm^2 were calculated, as well as the number of myelin layers per 100 nm, the length of the intraperiod line, and the g-ratio (axon diameter/axon diameter including myelin sheath).

4.14. Statistical Analysis

All data were analyzed and quantified by experimenters who were blind to the experimental design. Statistical analysis was performed using GraphPad Prism (San Diego, CA, USA). Statistical tests, posttests and significance values are indicated in figure legends. In all cases, α-value was set at 0.05.

5. Conclusions

We demonstrate a window of therapeutic opportunity and show that even late BMMC treatment in rats with transient peripheral nerve injury results in an immediate response to cell therapy, reflected in a gradual return to basal pain-like behavior and faster nerve regeneration in terms of morphology and functionality.

Author Contributions: Conceptualization, Vanina Usach and Patricia Setton-Avruj.; methodology, Vanina Usach and Patricia Setton-Avruj; investigation, Mailin Casadei and Pablo Brumovsky (mechanical and cold allodynia studies), Alicia Cueto (electrophysiological studies), Vanina Usach, Gonzalo Piñero, Marianela Vence, Paula Soto (rest of the experiments); validation, Vanina Usach and Patricia Setton-Avruj; resources, Patricia Setton-Avruj and Pablo Brumovsky; writing—original draft preparation, Vanina Usach; writing—review and editing, Patricia Setton-Avruj.; visualization, Vanina Usach; supervision, Patricia Setton-Avruj; project administration, Particia Setton-Avruj and Pablo Brumovsky; funding acquisition, Patricia Setton-Avruj and Pablo Brumovsky. All authors have read and agreed to the published version of the manuscript.

Funding: This research was funded by Agencia Nacional de Promoción Científica y Tecnológica (PICTO-Startup 2016-0091 and PICT 2017-0969, PICT 2017-3952, Universidad Austral (I-800201701000006UA-17), Universidad de Buenos Aires (UBACYT 20020170100588BA), and Consejo Nacional de Investigaciones Científicas y Técnicas (PIP 1059).

Institutional Review Board Statement: The study was approved by Comité de Bioética at Facultad de Farmacia y Bioquímica, Universidad de Buenos Aires (CICUAL 1488/19), the Institutional Animal Care and Use Committee (IACUC; 17-04) of the IIMT CONICET-Universidad Austral, and in accordance with the NIH Guide for the Care and Use of Laboratory Animals (NIH Publications 86-23), the Directive 2010/63/EU for animal experiments of the European Parliament and the Council of the European Union.

Data Availability Statement: data supporting these findings are available on reasonable request.

Acknowledgments: Ms. María Marta Rancez for her assistance in the elaboration of this manuscript.

Conflicts of Interest: The authors declare no conflicts of interest.

 doi:10.20944/preprints202405.0352.v1

References

1. Conforti, L.; Gilley, J.; Coleman, M.P. Wallerian Degeneration: An Emerging Axon Death Pathway Linking Injury and Disease. *Nat. Rev. Neurosci.* 2014, *15*, 394–409.
2. Gaudet, A.D.; Popovich, P.G.; Ramer, M.S. Wallerian Degeneration: Gaining Perspective on Inflammatory Events after Peripheral Nerve Injury. *J. Neuroinflammation* 2011, *8*.
3. Chen, P.; Piao, X.; Bonaldo, P. Role of Macrophages in Wallerian Degeneration and Axonal Regeneration after Peripheral Nerve Injury. *Acta Neuropathol.* 2015, *130*, 605–618.
4. Davies, A.J.; Kim, H.W.; Gonzalez-Cano, R.; Choi, J.; Back, S.K.; Roh, S.E.; Johnson, E.; Gabriac, M.; Kim, M.S.; Lee, J.; et al. Natural Killer Cells Degenerate Intact Sensory Afferents Following Nerve Injury. *Cell* **2019**, *176*, 716-728.e18, doi:10.1016/j.cell.2018.12.022.
5. Lancelotta, M.P.; Sheth, R.N.; Meyer, R.A.; Belzberg, A.J.; Griffin, J.W.; Campbell, J.N.; Kretschmer, T.; Richter, H.P.; Linderoth, B.; Huang, J.H.; et al. Severity and Duration of Hyperalgesia in Rat Varies with Type of Nerve Lesion. *Neurosurgery* **2003**, *53*, 1200–1209, doi:10.1227/01.NEU.0000089482.80879.9A.
6. Casals-Díaz, L.; Vivó, M.; Navarro, X. Nociceptive Responses and Spinal Plastic Changes of Afferent C-Fibers in Three Neuropathic Pain Models Induced by Sciatic Nerve Injury in the Rat. *Exp. Neurol.* **2009**, *217*, 84–95, doi:10.1016/j.expneurol.2009.01.014.
7. Segers, V.F.M.; Lee, R.T. Stem-Cell Therapy for Cardiac Disease. *Nature* 2008, *451*, 937–942.
8. Usach, V.; Malet, M.; López, M.; Lavalle, L.; Piñero, G.; Saccoliti, M.; Cueto, A.; Brumovsky, P.; Brusco, A.; Setton-Avruj, P. Systemic Transplantation of Bone Marrow Mononuclear Cells Promotes Axonal Regeneration and Analgesia in a Model of Wallerian Degeneration. *Transplantation* **2017**, *101*, doi:10.1097/TP.0000000000001478.
9. Guérout, N.; Duclos, C.; Drouot, L.; Abramovici, O.; Bon-Mardion, N.; Lacoume, Y.; Jean, L.; Boyer, O.; Marie, J.P. Transplantation of Olfactory Ensheathing Cells Promotes Axonal Regeneration and Functional Recovery of Peripheral Nerve Lesion in Rats. *Muscle and Nerve* **2011**, *43*, 543–551, doi:10.1002/mus.21907.
10. Yao Chang, M.; Han Chang, C.; Hsi Chen, C.; Cheng, B.; Dong Lin, Y.; Yau Luo, C.; Lin Wu, H.; Jen Yang, Y.; Hong Chen, J.; Hsieh, P.C.H. The Time Window for Therapy with Peptide Nanofibers Combined with Autologous Bone Marrow Cells in Pigs after Acute Myocardial Infarction. *PLoS One* **2015**, *10*, doi:10.1371/journal.pone.0115430.
11. Ishizaka, S.; Horie, N.; Satoh, K.; Fukuda, Y.; Nishida, N.; Nagata, I. Intra-Arterial Cell Transplantation Provides Timing-Dependent Cell Distribution and Functional Recovery after Stroke. *Stroke* **2013**, *44*, 720–726, doi:10.1161/STROKEAHA.112.677328.
12. Loubinoux, I.; Demain, B.; Davoust, C.; Plas, B.; Vaysse, L. Cellules Souches et Récupération Motrice Post-AV. *Ann. Phys. Rehabil. Med.* 2014, *57*, 499–508.
13. Li, Y.; Zhang, W.M.; Wang, T.H. Optimal Location and Time for Neural Stem Cell Transplantation into Transected Rat Spinal Cord. *Cell. Mol. Neurobiol.* **2011**, *31*, 407–414, doi:10.1007/s10571-010-9633-6.
14. Goel, R.K.; Suri, V.; Suri, A.; Sarkar, C.; Mohanty, S.; Sharma, M.C.; Yadav, P.K.; Srivastava, A. Effect of Bone Marrow-Derived Mononuclear Cells on Nerve Regeneration in the Transection Model of the Rat Sciatic Nerve. *J. Clin. Neurosci.* **2009**, *16*, 1211–1217, doi:10.1016/j.jocn.2009.01.031.
15. Lopes-Filho, J.D.; Caldas, H.C.; Santos, F.C.A.; Mazzer, N.; Simões, G.F.; Kawasaki-Oyama, R.S.; Abbud-Filho, M.; Oliveira, A.R.; Toboga, S.R.; Chueire, A.G. Microscopic Evidences That Bone Marrow Mononuclear Cell Treatment Improves Sciatic Nerve Regeneration after Neurorrhaphy. *Microsc. Res. Tech.* **2011**, *74*, 355–363, doi:10.1002/jemt.20916.
16. Raheja, A.; Suri, V.; Suri, A.; Sarkar, C.; Srivastava, A.; Mohanty, S.; Jain, K.G.; Sharma, M.C.; Mallick, H.N.; Yadav, P.K.; et al. Dose-Dependent Facilitation of Peripheral Nerve Regeneration by Bone Marrow-Derived Mononuclear Cells: A Randomized Controlled Study. Laboratory Investigation. *J. Neurosurg.* **2012**, *117*, 1170–1181, doi:10.3171/2012.8.JNS111446.
17. Donald Orlic[2], Jan Kajstura*, Stefano Chimenti*, Igor Jakoniuk*, Stacie M. Anderson[2], Baosheng Li*, James Pickel[3], Ronald McKay[3], Bernardo Nadal-Ginard*, David M. Bodine[2], A.L.& P.A. Bone Marrow Cells Regenerate Infarcted Myocardium. *Lett. to Nat.* **2001**, *410*, 701.
18. Holler, V.; Buard, V.; Roque, T.; Squiban, C.; Benderitter, M.; Flamant, S.; Tamarat, R. Early and Late Protective Effect of Bone Marrow Mononuclear Cell Transplantation on Radiation-Induced Vascular Dysfunction and Skin Lesions. *Cell Transplant.* **2019**, *28*, 116–128, doi:10.1177/0963689718810327.
19. Sharma, A.; Gokulchandran, N.; Sane, H.; Nagrajan, A.; Paranjape, A.; Kulkarni, P.; Shetty, A.; Mishra, P.; Kali, M.; Biju, H.; et al. Autologous Bone Marrow Mononuclear Cell Therapy for Autism: An Open Label Proof of Concept Study. *Stem Cells Int.* **2013**, doi:10.1155/2013/623875.
20. Huang, R.; Yao, K.; Sun, A.; Qian, J.; Ge, L.; Zhang, Y.; Niu, Y.; Wang, K.; Zou, Y.; Ge, J. Timing for Intracoronary Administration of Bone Marrow Mononuclear Cells after Acute ST-Elevation Myocardial Infarction: A Pilot Study. *Stem Cell Res. Ther.* **2015**, *6*, doi:10.1186/s13287-015-0102-5.
21. Assmus, B.; Alakmeh, S.; De Rosa, S.; Bönig, H.; Hermann, E.; Levy, W.C.; Dimmeler, S.; Zeiher, A.M. Improved Outcome with Repeated Intracoronary Injection of Bone Marrow-Derived Cells within a

Registry: Rationale for the Randomized Outcome Trial REPEAT. *Eur. Heart J.* **2016**, *37*, 1659–1666, doi:10.1093/eurheartj/ehv559.
22. Bhansali, A.; Upreti, V.; Khandelwal, N.; Marwaha, N.; Gupta, V.; Sachdeva, N.; Sharma, R.R.; Saluja, K.; Dutta, P.; Walia, R.; et al. Efficacy of Autologous Bone Marrow-Derived Stem Cell Transplantation in Patients with Type 2 Diabetes Mellitus. *Stem Cells Dev.* **2009**, *18*, 1407–1415, doi:10.1089/scd.2009.0164.
23. Madaric, J.; Klepanec, A.; Valachovicova, M.; Mistrik, M.; Bucova, M.; Olejarova, I.; Necpal, R.; Madaricova, T.; Paulis, L.; Vulev, I. Characteristics of Responders to Autologous Bone Marrow Cell Therapy for No-Option Critical Limb Ischemia. *Stem Cell Res. Ther.* **2016**, *7*, doi:10.1186/s13287-016-0379-z.
24. Daltro, G.C.; Fortuna, V.; De Souza, E.S.; Salles, M.M.; Carreira, A.C.; Meyer, R.; Freire, S.M.; Borojevic, R. Efficacy of Autologous Stem Cell-Based Therapy for Osteonecrosis of the Femoral Head in Sickle Cell Disease: A Five-Year Follow-up Study. *Stem Cell Res. Ther.* **2015**, *6*, doi:10.1186/s13287-015-0105-2.
25. Ismail, A.M.; Abdou, S.M.; Abdelnaby, A.Y.; Hamdy, M.A.; El Saka, A.A.; Gawaly, A. Stem Cell Therapy Using Bone Marrow-Derived Mononuclear Cells in Treatment of Lower Limb Lymphedema: A Randomized Controlled Clinical Trial. *Lymphat. Res. Biol.* **2018**, *16*, 270–277, doi:10.1089/LRB.2017.0027.
26. Suzuki, Y.; Ishikawa, N.; Omae, K.; Hirai, T.; Ohnishi, K.; Nakano, N.; Nishida, H.; Nakatani, T.; Fukushima, M.; Ide, C. Bone Marrow-Derived Mononuclear Cell Transplantation in Spinal Cord Injury Patients by Lumbar Puncture. *Restor. Neurol. Neurosci.* **2014**, *32*, 473–482, doi:10.3233/RNN-130363.
27. Setton-Avruj, C.P.; Musolino, P.L.; Salis, C.; Alló, M.; Bizzozero, O.; Villar, M.J.; Soto, E.F.; Pasquini, J.M. Presence of α-Globin MRNA and Migration of Bone Marrow Cells after Sciatic Nerve Injury Suggests Their Participation in the Degeneration/Regeneration Process. *Exp. Neurol.* **2007**, *203*, 568–578, doi:10.1016/j.expneurol.2006.09.024.
28. Piñero, G.; Usach, V.; Soto, P.A.; Monje, P. V.; Setton-Avruj, P. EGFP Transgene: A Useful Tool to Track Transplanted Bone Marrow Mononuclear Cell Contribution to Peripheral Remyelination. *Transgenic Res.* **2018**, *27*, 135–153, doi:10.1007/S11248-018-0062-5.
29. Usach, V.; Goitia, B.; Lavalle, L.; Martinez Vivot, R.; Setton-Avruj, P. Bone Marrow Mononuclear Cells Migrate to the Demyelinated Sciatic Nerve and Transdifferentiate into Schwann Cells after Nerve Injury: Attempt at a Peripheral Nervous System Intrinsic Repair Mechanism. *J. Neurosci. Res.* **2011**, *89*, 1203–1217, doi:10.1002/jnr.22645.
30. Gomez-Sanchez, J.A.; Carty, L.; Iruarrizaga-Lejarreta, M.; Palomo-Irigoyen, M.; Varela-Rey, M.; Griffith, M.; Hantke, J.; Macias-Camara, N.; Azkargorta, M.; Aurrekoetxea, I.; et al. Schwann Cell Autophagy, Myelinophagy, Initiates Myelin Clearance from Injured Nerves. *J. Cell Biol.* **2015**, *210*, 153–168, doi:10.1083/jcb.201503019.
31. Jessen, K.R.; Arthur-Farraj, P. Repair Schwann Cell Update: Adaptive Reprogramming, EMT, and Stemness in Regenerating Nerves. *Glia* 2019, *67*, 421–437.
32. Nocera, G.; Jacob, C. Mechanisms of Schwann Cell Plasticity Involved in Peripheral Nerve Repair after Injury. *Cell. Mol. Life Sci.* **2020**, *77*, 3977–3989, doi:10.1007/S00018-020-03516-9.
33. Chen, F.; Suzuki, Y.; Nagai, N.; Peeters, R.; Coenegrachts, K.; Coudyzer, W.; Marchal, G.; Ni, Y. Visualization of Stroke with Clinical MR Imagers in Rats: A Feasibility Study. *Radiology* **2004**, *233*, 905–911, doi:10.1148/radiol.2333031658.
34. Yang, B.; Strong, R.; Sharma, S.; Brenneman, M.; Mallikarjunarao, K.; Xi, X.; Grotta, J.C.; Aronowski, J.; Savitz, S.I. Therapeutic Time Window and Dose Response of Autologous Bone Marrow Mononuclear Cells for Ischemic Stroke. *J. Neurosci. Res.* **2011**, *89*, 833–839, doi:10.1002/jnr.22614.
35. de Vasconcelos dos Santos, A.; da Costa Reis, J.; Diaz Paredes, B.; Moraes, L.; Jasmin; Giraldi-Guimarães, A.; Mendez-Otero, R. Therapeutic Window for Treatment of Cortical Ischemia with Bone Marrow-Derived Cells in Rats. *Brain Res.* **2010**, *1306*, 149–158, doi:10.1016/j.brainres.2009.09.094.
36. Tamura, K.; Harada, Y.; Kunimi, M.; Takemitsu, H.; Hara, Y.; Nakamura, T.; Tagawa, M. Autologous Bone Marrow Mononuclear Cell Transplant and Surgical Decompression in a Dog with Chronic Spinal Cord Injury. *Exp. Clin. Transplant.* **2015**, *13*, 100–105, doi:10.6002/ect.2013.0237.
37. Tamura, K.; Maeta, N. Efficacy of Autologous Bone Marrow Mononuclear Cell Transplantation in Dogs with Chronic Spinal Cord Injury. *Open Vet. J.* **2020**, *10*, 206–215, doi:10.4314/OVJ.V10I2.10.
38. do Prado-Lima, P.A.S.; Onsten, G.A.; de Oliveira, G.N.; Brito, G.C.; Ghilardi, I.M.; de Souza, E.V.; dos Santos, P.G.; Salamoni, S.D.; Machado, D.C.; Duarte, M.M.F.; et al. The Antidepressant Effect of Bone Marrow Mononuclear Cell Transplantation in Chronic Stress. *J. Psychopharmacol.* **2019**, doi:10.1177/0269881119841562.
39. Costa-Ferro, Z.S.M.; do Prado-Lima, P.A.S.; Onsten, G.A.; Oliveira, G.N.; Brito, G.C.; Ghilardi, I.M.; dos Santos, P.G.; Bertinatto, R.J.; da Silva, D.V.; Salamoni, S.D.; et al. Bone Marrow Mononuclear Cell Transplant Prevents Rat Depression and Modulates Inflammatory and Neurogenic Molecules. *Prog. Neuropsychopharmacol. Biol. Psychiatry* **2022**, *113*, doi:10.1016/J.PNPBP.2021.110455.
40. Lutz, A.B.; Chung, W.S.; Sloan, S.A.; Carson, G.A.; Zhou, L.; Lovelett, E.; Posada, S.; Zuchero, J.B.; Barres, B.A. Schwann Cells Use TAM Receptor-Mediated Phagocytosis in Addition to Autophagy to Clear Myelin

in a Mouse Model of Nerve Injury. *Proc. Natl. Acad. Sci. U. S. A.* **2017**, *114*, E8072–E8080, doi:10.1073/pnas.1710566114.

41. Li, R.; Li, D.; Wu, C.; Ye, L.; Wu, Y.; Yuan, Y.; Yang, S.; Xie, L.; Mao, Y.; Jiang, T.; et al. Nerve Growth Factor Activates Autophagy in Schwann Cells to Enhance Myelin Debris Clearance and to Expedite Nerve Regeneration. *Theranostics* **2020**, *10*, 1649–1677, doi:10.7150/THNO.40919.
42. Sheu, M.L.; Cheng, F.C.; Su, H.L.; Chen, Y.J.; Chen, C.J.; Chiang, C.M.; Chiu, W.T.; Sheehan, J.; Pan, H.C. Recruitment by SDF-1α of CD34-Positive Cells Involved in Sciatic Nerve Regeneration: Laboratory Investigation. *J. Neurosurg.* **2012**, *116*, 432–444, doi:10.3171/2011.3.JNS101582.
43. Jander, S.; Lausberg, F.; Stoll, G. Differential Recruitment of CD8+ Macrophages during Wallerian Degeneration in the Peripheral and Central Nervous System. *Brain Pathol.* **2001**, *11*, 27–38, doi:10.1111/J.1750-3639.2001.TB00378.X.
44. Moalem, G.; Monsonego, A.; Shani, Y.; Cohen, I.R.; Schwartz, M. *Differential T Cell Response in Central and Peripheral Nerve Injury: Connection with Immune Privilege*; 1999; Vol. 13;.
45. Carr, M.J.; Toma, J.S.; Johnston, A.P.W.; Steadman, P.E.; Yuzwa, S.A.; Mahmud, N.; Frankland, P.W.; Kaplan, D.R.; Miller, F.D. Mesenchymal Precursor Cells in Adult Nerves Contribute to Mammalian Tissue Repair and Regeneration. *Cell Stem Cell* **2019**, *24*, 240-256.e9, doi:10.1016/j.stem.2018.10.024.
46. Clements, M.P.; Byrne, E.; Camarillo Guerrero, L.F.; Cattin, A.L.; Zakka, L.; Ashraf, A.; Burden, J.J.; Khadayate, S.; Lloyd, A.C.; Marguerat, S.; et al. The Wound Microenvironment Reprograms Schwann Cells to Invasive Mesenchymal-like Cells to Drive Peripheral Nerve Regeneration. *Neuron* **2017**, *96*, 98-114.e7, doi:10.1016/j.neuron.2017.09.008.
47. Nadeau, S.; Filali, M.; Zhang, J.; Kerr, B.J.; Rivest, S.; Soulet, D.; Iwakura, Y.; Vaccari, J.P. de R.; Keane, R.W.; Lacroix, S. Functional Recovery after Peripheral Nerve Injury Is Dependent on the Pro-Inflammatory Cytokines IL-1β and TNF: Implications for Neuropathic Pain. *J. Neurosci.* **2011**, *31*, 12533–12542, doi:10.1523/JNEUROSCI.2840-11.2011.
48. Sharma, A.; Hemangi Sane; Nandini Gokulchandran; Pooja Kulkarni; Alitta Jose; Vivek Nair; Rohit Das; Vaibhav Lakhanpal; Prerna Badhe Intrathecal Transplantation of Autologous Bone Marrow Mononuclear Cells in Patients with Sub-Acute and Chronic Spinal Cord Injury: An Open-Label Study. *Int. J. Health Sci. (Qassim).* **2020**, 24–32.
49. Sharma, A.K.; Sane, H.M.; Kulkarni, P.P.; Gokulchandran, N.; Biju, H.; Badhe, P.B. Autologous Bone Marrow Mononuclear Cell Transplantation in Patients with Chronic Traumatic Brain Injury- a Clinical Study. *Cell Regen. (London, England)* **2020**, *9*, 3, doi:10.1186/s13619-020-00043-7.
50. Naruse, K.; Sato, J.; Funakubo, M.; Hata, M.; Nakamura, N.; Kobayashi, Y.; Kamiya, H.; Shibata, T.; Kondo, M.; Himeno, T.; et al. Transplantation of Bone Marrow-Derived Mononuclear Cells Improves Mechanical Hyperalgesia, Cold Allodynia and Nerve Function in Diabetic Neuropathy. *PLoS One* **2011**, *6*, doi:10.1371/journal.pone.0027458.
51. Takamura, H.; Terashima, T.; Mori, K.; Katagi, M.; Okano, J.; Suzuki, Y.; Imai, S.; Kojima, H. Bone-Marrow-Derived Mononuclear Cells Relieve Neuropathic Pain after Spinal Nerve Injury in Mice. *Mol. Ther. - Methods Clin. Dev.* **2020**, *17*, 657–665, doi:10.1016/j.omtm.2020.03.020.
52. Song, F.; Tang, J.; Geng, R.; Hu, H.; Zhu, C.; Cui, W.; Fan, W. *Comparison of the Efficacy of Bone Marrow Mononuclear Cells and Bone Mesenchymal Stem Cells in the Treatment of Osteoarthritis in a Sheep Model*; 2014; Vol. 7;.
53. Cuende, N.; Rico, L.; Herrera, C. Concise Review: Bone Marrow Mononuclear Cells for the Treatment of Ischemic Syndromes: Medicinal Product or Cell Transplantation? *Stem Cells Transl. Med.* **2012**, *1*, 403–408, doi:10.5966/SCTM.2011-0064.
54. Takahashi, M.; Li, T.S.; Suzuki, R.; Kobayashi, T.; Ito, H.; Ikeda, Y.; Matsuzaki, M.; Hamano, K. Cytokines Produced by Bone Marrow Cells Can Contribute to Functional Improvement of the Infarcted Heart by Protecting Cardiomyocytes from Ischemic Injury. *Am. J. Physiol. Heart Circ. Physiol.* **2006**, *291*, doi:10.1152/AJPHEART.00142.2006.
55. Thrasivoulou, C.; Soubeyre, V.; Ridha, H.; Giuliani, D.; Giaroni, C.; Michael, G.J.; Saffrey, M.J.; Cowen, T. Reactive Oxygen Species, Dietary Restriction and Neurotrophic Factors in Age-Related Loss of Myenteric Neurons. *Aging Cell* **2006**, *5*, 247–257, doi:10.1111/j.1474-9726.2006.00214.x.
56. Okano, H.; Ogawa, Y.; Nakamura, M.; Kaneko, S.; Iwanami, A.; Toyama, Y. Transplantation of Neural Stem Cells into the Spinal Cord after Injury. *Semin. Cell Dev. Biol.* **2003**, *14*, 191–198, doi:10.1016/S1084-9521(03)00011-9.
57. Huang, P.C.; Tsai, K.L.; Chen, Y.W.; Lin, H.T.; Hung, C.H. Exercise Combined With Ultrasound Attenuates Neuropathic Pain in Rats Associated With Downregulation of IL-6 and TNF-α, but With Upregulation of IL-10. *Anesth. Analg.* **2017**, *124*, 2038–2044, doi:10.1213/ANE.0000000000001600.
58. Piñero, G.; Vence, M.; Aranda, M.L.; Cercato, M.C.; Soto, P.A.; Usach, V.; Setton-Avruj, P.C. All the PNS Is a Stage: Transplanted Bone Marrow Cells Play an Immunomodulatory Role in Peripheral Nerve Regeneration. *ASN Neuro* **2023**, *15*, doi:10.1177/17590914231167281.

59. Mapplebeck, J.C.S.; Beggs, S.; Salter, M.W. Sex Differences in Pain: A Tale of Two Immune Cells. *Pain* **2016**, *157 Suppl 1*, S2–S6, doi:10.1097/J.PAIN.0000000000000389.
60. Ramachandran, R.; Wang, Z.; Saavedra, C.; DiNardo, A.; Corr, M.; Powell, S.B.; Yaksh, T.L. Role of Toll-like Receptor 4 Signaling in Mast Cell-Mediated Migraine Pain Pathway. *Mol. Pain* **2019**, *15*, doi:10.1177/1744806919867842.
61. Stokes, J.A.; Cheung, J.; Eddinger, K.; Corr, M.; Yaksh, T.L. Toll-like Receptor Signaling Adapter Proteins Govern Spread of Neuropathic Pain and Recovery Following Nerve Injury in Male Mice. *J. Neuroinflammation* **2013**, *10*, 10–13, doi:10.1186/1742-2094-10-148.
62. Kanaya, F.; Firrell, J.C.; Breidenbach, W.C. Sciatic Function Index, Nerve Conduction Tests, Muscle Contraction, and Axon Morphometry as Indicators of Regeneration. *Plast. Reconstr. Surg.* **1996**, *98*, 1264–1274, doi:10.1097/00006534-199612000-00023.
63. Dellon, A.L.; Mackinnon, S.E. Selection of the Appropriate Parameter to Measure Neural Regeneration. *Ann. Plast. Surg.* **1989**, *23*, 197–202, doi:10.1097/00000637-198909000-00002.
64. Wang, T.; Ito, A.; Aoyama, T.; Nakahara, R.; Nakahata, A.; Ji, X.; Zhang, J.; Kawai, H.; Kuroki, H. Functional Evaluation Outcomes Correlate with Histomorphometric Changes in the Rat Sciatic Nerve Crush Injury Model: A Comparison between Sciatic Functional Index and Kinematic Analysis. *PLoS One* **2018**, *13*, doi:10.1371/journal.pone.0208985.
65. Munro, C.A.; Szalai, J.P.; Mackinnon, S.E.; Midha, R. *LACK OF ASSOCIATION BETWEEN OUTCOME MEASURES OF NERVE REGENERATION*; 1998; Vol. 21;.
66. Monte-Raso, V.V.; Barbieri, C.H.; Mazzer, N.; Yamasita, A.C.; Barbieri, G. Is the Sciatic Functional Index Always Reliable and Reproducible? *J. Neurosci. Methods* **2008**, *170*, 255–261, doi:10.1016/j.jneumeth.2008.01.022.
67. Nguyen, T.L.; Nguyen, H.P.; Nguyen, T.K. The Effects of Bone Marrow Mononuclear Cell Transplantation on the Quality of Life of Children with Cerebral Palsy. *Health Qual. Life Outcomes* **2018**, *16*, doi:10.1186/s12955-018-0992-x.
68. Chaplan, S.R.; Bach, F.W.; Pogrel, J.W.; Chung, J.M.; Yaksh, T.L. *Quantitative Assessment of Tactile Allodynia in the Rat Paw*; 1994; Vol. 53;.
69. Choi, Y.; Wook Yoon, Y.; Sik Na, H.; Ho Kim, S.; Chung, J.M. *Behavioral Signs of Ongoing Pain and Cold Allodynia in a Rat Model of Neuropathic Pain*; 1994; Vol. 59;.
70. Kim, H.; Park, J.S.; Yong, J.C.; Kim, M.O.; Yang, H.H.; Kim, S.W.; Ji, W.H.; Lee, J.Y.; Kim, S.; Houge, M.A.; et al. Bone Marrow Mononuclear Cells Have Neurovascular Tropism and Improve Diabetic Neuropathy. *Stem Cells* **2009**, *27*, 1686–1696, doi:10.1002/stem.87.
71. Hruskal, R.E.; Kennedy, S.; Silbergeld, E.K. *QUANTITATIVE ASPECTS OF NORMAL LOCOMOTION IN RATS*; Pergamon Press, 1979; Vol. 25;.
72. MM, B. A Rapid and Sensitive Method for the Quantitation of Microgram Quantities of Protein Utilizing the Principle of Protein-Dye Binding. *Anal. Biochem.* **1976**, *72*, 248–254, doi:10.1006/ABIO.1976.9999.
73. Saper, C.B. An Open Letter to Our Readers on the Use of Antibodies. *J. Comp. Neurol.* **2005**, *493*, 477–478, doi:10.1002/CNE.20839.
74. Esparza, M.A.; Bollati, F.; Garcia-Keller, C.; Virgolini, M.B.; Lopez, L.M.; Brusco, A.; Shen, H.W.; Kalivas, P.W.; Cancela, L.M. Stress-Induced Sensitization to Cocaine: Actin Cytoskeleton Remodeling within Mesocorticolimbic Nuclei. *Eur. J. Neurosci.* **2012**, *36*, 3103–3117, doi:10.1111/J.1460-9568.2012.08239.X.